

Sensing with Memristive Complementary Resistive Switch: Modelling and Simulations

Vishal Gupta*, Danilo Pellegrini*, Saurabh Khandelwal[†], Abusaleh Jabir[‡],
Shahar Kvatinsky[‡], Eugenio Martinelli*, Corrado Di Natale*, and Marco Ottavi*

*Electronic Engineering, University of Rome “Tor Vergata”, Italy. Email: vishal.gupta@students.uniroma2.eu,
danilo.pellegrini@alumni.uniroma2.eu, {martinelli, dinatale, ottavi}@ing.uniroma2.it

[†]School of ECM, Oxford Brookes University, UK. Email: {skhandelwal, ajabir}@brookes.ac.uk

[‡]Technion - Israel Institute of Technology, Haifa, Israel. Email: shahar@ee.technion.ac.il

Abstract—Sensors give factual and process information about the environment or other physical phenomena. Sensing using memristors has been recently introduced for its potential for high density integration and miniaturization. Complementary Resistive Switch (CRS) based sensor provides an extremely efficient crossbar array that reduces the sneak current. The objective of this paper is to introduce and evaluate a circuit model for sensing using memristive complementary resistive switch. We introduce a reliable SPICE implementation of memristor model that captures the sensing behaviour of memristor. Our simulation results also validate the SPICE model for CRS sensing architecture, whose parameters could be easily adapted to match experimental data. The results also investigate the sensitivity and device behaviour of memristor and CRS sensor device in the presence of oxidizing and reducing gases of different concentration.

I. INTRODUCTION

Leon O. Chua introduced the theoretical concept of memristor in 1971 [1] and the HP Laboratories revealed the first physical device of memristor in 2008 [2]. Since then, many memristors based applications have been fabricated to suit their targets such as memory [2], computing [3], logic [4], artificial neural networks [5], and impedance matching network [6]. Memristors are by no means hard to fabricate and are made out of nanoimprint lithography, which is a low cost process [7].

Recently memristive devices demonstrated gas sensing properties [8], [9], [10]. The resistance of the memristor e.g. in a TiO_2 based device is determined by the resistance of an undoped region (TiO_2) and of a doped region (TiO_{2-x}). The structure of a typical TiO_2 -based memristor is shown in Fig. 1a [2]. TiO_2 is regarded as a reliable gas sensor because of its better response rate, low cost, fast response time and stability [11], [12]. To allow the interaction, the top terminal of the physical memristor based sensor is left partially uncovered as shown in Fig. 1b and the direction of the change in resistance depends on the type of the gas exposed. Also, the change in resistivity takes place without affecting the position of the device’s state variable x , as long as the device is in the ‘hold’ state during sensing [8], [10].

Array of sensors also open up the possibility to detect, quantify and differentiate multiple gases in real time [13]. In traditional approaches, bidirectional flow of current in oxide-based memristors causes sneak path leading to erroneous sensing in sensor crossbar architecture. This is mostly due to the formation of a parallel resistance path between resistance of unselected cells and the desired cell(s) [14]. Several

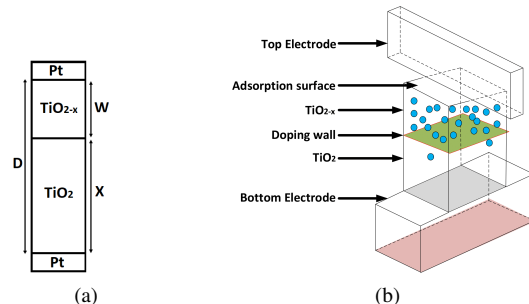


Figure 1: (a) Schematic of TiO_2 -based memristor device. (b) Cross-section view of a memristor device for sensing applications [13].

approaches were explored in [13], [15] to minimize the sneak path current but had several disadvantages. For example in [15], if one of the faulty sensors in the crossbar exhibits a very low resistance, the output voltage is altered drastically and it become very difficult to identify the faulty sensor in a larger array. In [13], 1T1M architecture interposes a MOSFET transistor between the sensing memristor and the row, enabling and disabling the connection of the sensor to the circuit. However, MOSFET transistors show short channel effects at lower technology nodes [16]. Hence, an efficient solution needs to be proposed to strongly reduce the sneak currents (parasitic currents) in memristor based arrays.

Complementary resistive switch (CRS) device is used to avoid sneak-path currents in the architecture, which consist of two anti-serial memristive elements. Also, CRS due to their usability as a sensor fit the requirements for improved sensing. Based on this, we present a CRS sensor in an attempt to reduce the challenges posed by current leakages in memristive arrays. The CRS is a combination of two anti-serially connected memristors, 1 and 2, as shown in the left side of Fig. 2. The I-V curve of the CRS device is divided in traits as shown in right side of Fig. 2. Here, the sign $1H/2L$ signifies that the memristor 1 is in high resistance state (HRS) and the memristor 2 is in low resistance state (LRS). A consistent flow of current is observed in both positive and negative biased applied voltage, when both memristors are set to LRS.

The CRS sensing architecture shown in Fig. 3 is composed of access memristors and sensors. The sensors S exhibits LRS state while access memristors exhibits either HRS or LRS state. The functionality of the access memristors is to disconnect the devices which are not connected during a read

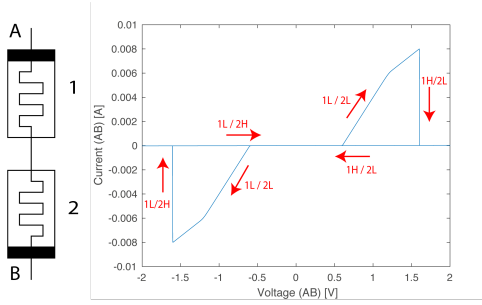


Figure 2: Left side shows two memristors in connected anti-serially to form a CRS device where negative electrode of the memristors presents by black colored trait. On the right side, the I-V characteristics showing CRS behaviour.

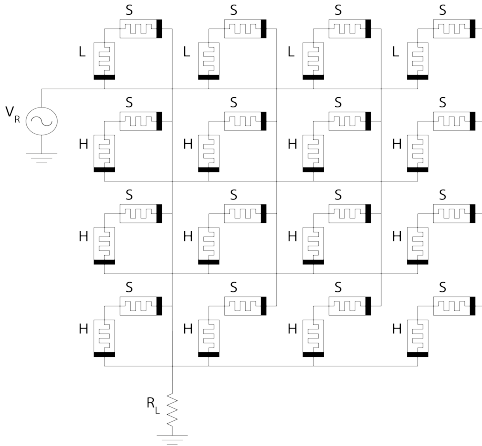


Figure 3: A 4×4 size CRS sensor crossbar array. Here, S represents the sensor, L and H denote the low and high resistive states of the memristor respectively [17].

operation. To read the corresponding row after the exposure of the gas, the access memristors in that row are configured to LRS while the other access memristors are configured to HRS. This drastically minimizes the sneak path effects by reducing the flow of the current through un-selected cells [17].

This paper is an extension of our previous work presented in [17] that introduced a novel multi-sensing structure, namely CRS sensing (Fig. 3) that significantly minimizes the sneak path current in a crossbar array. However, this paper focuses on sensing behaviour of CRS crossbar array in the presence of reducing and oxidising gases. The proposed architecture reduces measurement error by taking multiple measurements and provide an ultra-dense circuitual solution for sensing. The main contributions of this paper are as follows:

- 1) A simplified VTEAM based SPICE gas sensor model and its validation through simulation results.
- 2) Comparison of the proposed gas sensor model with previously reported models.
- 3) Investigating the behaviour of the memristor based sensor and CRS sensor device for different concentration of gases.
- 4) Examining the sensitivity of CRS sensors device in a CRS sensing crossbar array.

The rest of the paper is organized as follows: Section 2 de-

scribe simplified SPICE modelling for gas sensing application and comparison to the pre-existing sensing models. Section 3 demonstrate simulation results to examine the sensitivity of single memristor device and CRS device as a gas sensor in CRS sensing architecture in different gases environment with various concentrations. The paper is concluded in Section 4.

II. SPICE MODELLING FOR SENSING

A. SPICE Modelling

Our previous study for CRS gas sensing approach has been discussed and modeled by the Yakopcic sensing model presented in [17]. Here, we report a detail study for sensing mechanism and the device behaviour in different environment of gases for CRS sensing architecture. A Voltage ThrEshold Adaptive Model (VTEAM) model has been proposed for SPICE simulation in simplified way as compared to the model presented in the [18]. This model has been verified by the simulation of the memristor gas sensing behaviour, which was not done in [18].

Our gas sensing model is mainly inspired by the model presented in the [19], we converted the mathematical functions into SPICE circuitual code and adding the functions for sensing. One of the advantages of the VTEAM approach is based on voltage thresholds, unlike the previous characterizations reported in [20], [21], [22], and apart from this, the greater fidelity [19] to the real device behavior allows us to accurately design and simulate logic based circuits with memristors [23]. Our VTEAM model also has advantages as we have shorter computational times, generic behaviour, sufficient accuracy for the practical memristive device and less complexity [22] as compared to the previously reported sensing model presented in the [13], [17], [18]. All the simulation has been performed by using LTSpice simulator as it has an intuitive interface and able to see netlist by circuit designer, easy to use, and its free accessibility.

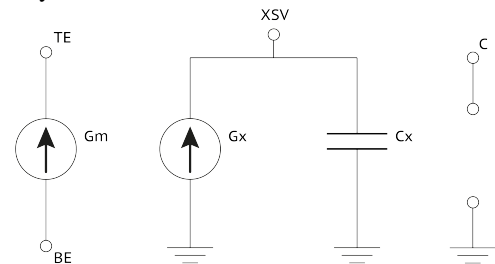


Figure 4: Electronic sub-circuit for proposed gas sensing model.

The model sub-circuit structure is similar to the Yakopcic model, with the addition of a pin C , as shown in Fig. 4. The pin C is externally connected to a voltage source representing the gas concentration in parts per million (PPM). Internally, it is only meant to probe having a voltage with respect to ground and applied input across these terminal and changes the final value of the memristance. The main differences between models reside in the functions controlling the derivative of the state variable and the conductance of the device. Here, the derivative of the state variable is associated to G_x . The conductance of the device is associated to the G_m and multiplied by the applied voltage. To make VTEAM more

consistent with the generally accepted polarization notation, we reversed the role of the voltage thresholds defined in [19], implicitly reversing the disposition of the device's electrodes too. The derivative of the state variable is defined by the following relationship, presented in equation (1):

$$\frac{dx(t)}{dt} = \begin{cases} K_{on} \cdot \left(\frac{V(t)}{V_{on}} - 1\right)^{\alpha_{on}} \cdot f(x), & V(t) > V_{on} \quad (1a) \\ 0, & V_{off} \leq V(t) \leq V_{on} \quad (1b) \\ K_{off} \cdot \left(\frac{V(t)}{V_{off}} - 1\right)^{\alpha_{off}} \cdot f(x), & V(t) < V_{off} \quad (1c) \end{cases}$$

We have set up the value of V_{on} and V_{off} on positive and negative scale respectively. The state variable x is here bounded between $[x_{on}, x_{off}]$ (thanks to the nullifying action of $f(x)$), meaning that when $x = x_{on}$ we have the low resistance state, and the high resistance state when $x = x_{off}$ (note that $x_{on} < x_{off}$). Parameters K_{on} & K_{off} are constant and the values are negative & positive respectively. Also, parameters α_{on} & α_{off} both are constant and whose values are greater than or equal to 1. Here, $x(t)$ is the state variable, corresponding to the voltage on the XSV terminal (that must be left floating outside the sub-circuit). $V(t)$ is the voltage across TE and BE terminals. The I-V relationship changes by following the trend of the state variable, representing by the equation (2), as shown below:

$$I_{Gm}(t) = V(t) \cdot \left[R_{eff} + \frac{R_{off} - R_{eff}}{x_{off} - x_{on}} \cdot (x - x_{on}) \right]^{-1} \quad (2)$$

and specifically:

$$I_{Gm}(t) = \begin{cases} \frac{V(t)}{R_{eff}}, & \text{if } x = x_{on} \quad (3a) \\ \frac{V(t)}{R_{off}}, & \text{if } x = x_{off} \quad (3b) \end{cases}$$

where parameters R_{off} , x_{on} and x_{off} provided in the same manner as in the [19], while R_{eff} substitutes the R_{on} parameter to include the sensing dynamics in (2). By adapting the modification for sensing, R_{eff} is defined as:

$$R_{eff} = \begin{cases} \frac{R_{on}}{1 + A \cdot V_C^\beta} & \text{for ox. gas} \quad (4a) \\ R_{on} \cdot (1 + A \cdot V_C^\beta) & \text{for red. gas} \quad (4b) \end{cases}$$

where, V_C represents the voltage applied on the C pin which also shows the gas concentration, A is the sensitivity coefficient and β is the response order for the subject gas. Our analysis only consider the instantaneous change in the resistance due to the missing time response analysis and experimental data of practical sensor device in the gas environment. Here, function $f(x)$ represents a window function, also authors in [19] suggest a free choice of settings among different proposed options for window function. We choose to implement a modified version of the Biolek window function [20], as it is intuitive, efficient and it aborts any stagnation effects of x at its boundaries (differently from the window function in [24]).

$$f(x) = 1 - \left[\frac{x - x_{on}}{x_{off} - x_{on}} - stp(v) \right]^{2p} \quad (5)$$

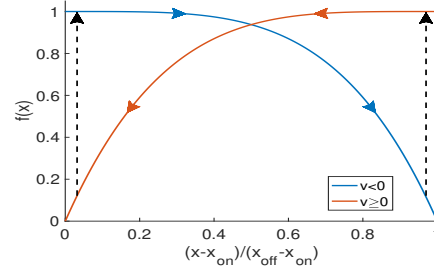


Figure 5: Window function for gas sensing model.

Where, stp is the step function given by the following equation:

$$stp(v) = \begin{cases} 1 & \text{if } v \geq 0 \quad (6a) \\ 0 & \text{if } v < 0 \quad (6b) \end{cases}$$

Two cases show trend of the Biolek window function when x is moving in opposite directions. The voltages applied (v) for the two curves have opposite signs too, so that the contributions of the stp function are different, presented in equation (6a) & (6b). On the axis of the abscissas, x is reported in a form where is first subtracted of the lowest allowed value, and then normalized, as in (5). The chosen value for p is 2. The black dashed arrows indicate the instantaneous changes in $f(x)$.

The window function presented in equation (5) becomes 0 when the state variable reaches one of the boundaries (x_{off} or x_{on}) and immediately becomes 1 when, once being in a certain boundary and x starts to move to the opposite direction. Since in VTEAM the state variable x gets lower when going to ON state and gets higher when going to OFF state, oppositely to what happens in [20], we took the argument of the window function positive instead of negative. We considered the voltage in place of the current flowing through, since VTEAM model is voltage-controlled and not current-controlled. This window function is plotted in Fig. 5. The SPICE code of this modified VTEAM model for sensing is reported in the appendix section at the end of the paper.

B. Comparison of models

Here, we are summarizing and comparing all the possible alternatives to simulate the gas sensing behaviour for memristor element. The very first proposed memristor model for gas sensing was presented in [13], by embedding the sensing mechanism into the HP memristor model, in addition to the Biolek window function. This sensing model presented in Verilog-A code and the same used for all the simulations. Here, state variable controlled by the current and non-linear voltage control mechanism of the state variable allows symmetric switching behavior. A major limitation of this approach is attributable to an absence of implementation of fixed threshold voltages. Practically, the memristance of the device changes even for very small voltages applied, in contrast with the several experimental evidences referenced in [19], [25]. Another issue is the poor adaptability to fit different real memristive devices, in which the Yakopcic and VTEAM model do not fail [22]. Also, in the case of Yakopcic [17] and proposed VTEAM based sensing model state variable controlled through the voltage.

Table I: Comparison between memristor sensing models.

Model for sensing	HP Model [13]	Yakopcic Model [25]	Our Model
State variable	$0 \leq x \leq D$	$0 \leq x \leq 1$	$x_{on} \leq x \leq x_{off}$
Voltage thresholds	Absent	Present	Present
Complexity	Medium	High	Low
$\frac{dx}{dt}$ - v relationship	\sinh	\exp	Polynomial
Generality & Flexibility	Low	Medium	High
Suitability for sensing	Low	Low	High

In Yakopcic based sensing model, change in state variable limited by an exponential function and also decaying with the rate of function $f(x)$. As simply, increasing the state variable results decreasing the device resistance. In comparison to the previous gas sensing models with our proposed VTEAM based SPICE model, the increases the resistance while moving the state variable towards the boundary. State variable x does not make any significant change with respect to the gas concentration in all the models as we have considered in this article for our comparative study. The gas concentration make only change in the value of R_{on} . At the same time, what makes VTEAM preferable respect to the Yakopcic model is the lower degree of complexity due to its simpler mathematical equations, which make it more appropriate for our sensing simulations and lighter in terms of computational processing. Table I shows the comparative analysis between previously proposed models and our VTEAM based SPICE model for gas sensing application.

III. SIMULATION RESULTS

A. Single memristor device as a gas sensor element

Here, analysis of gas sensing behaviour for a single memristor device has been presented and simulations have been done by the proposed SPICE model. Memristor behaviour as a gas sensor element has been observed in oxidizing and reducing gas environment with various concentration of gases. Simulation results show the validation of our proposed model for the memristor device and as a gas sensor element, which was missing in our previous analysis for sensing model in [18]. Fig. 6a shows the schematic of circuit diagram that were used in the analysis for the device behaviour, it consist of a memristor, in contact with gas, connected in series with a sinusoidal voltage source. These simulations explore the dual resistance of the memristor in a direct way. With the application of a voltage above a certain positive value (PTV), the inclination of the I-V curve increases since the device switches on; the opposite happens for a certain negative voltage (NTV). We plotted several I-V hysteresis curves, in each one the slope in the ON-state changes due to the interaction with an arbitrary unit (a. u.) i.e. parts per million (PPM) of gas. To validate our proposed model for the sensing behaviour, we have simulated memristor model without gases and with oxidizing & reducing

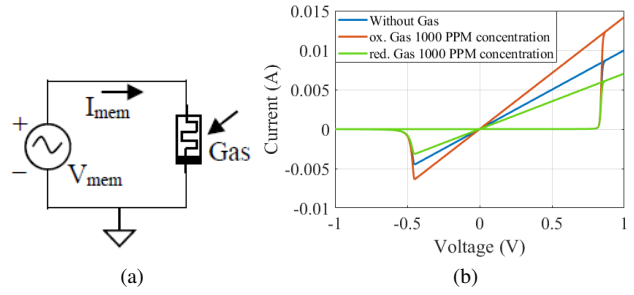


Figure 6: (a) Schematic of a memristor based single cell gas sensor. (b) I-V hysteresis curves showing variation in device resistance for without gas and with 1000 PPM of concentration for oxidizing & reducing gases.

gas environment. Fig. 6b displays simulation results which demonstrate the change in the ON-resistance of the memristor device, ON-resistance of the device decreases & increases in oxidizing and reducing gas environment for the 1000 PPM of gas concentration, respectively. Mathematically, change in the device resistance can be easily evaluated from the equations (4a) & (4b) and represented by the R_{eff} .

Initially, we analyzed the memristance of the device for no gas concentration called initial resistance which depends upon the device internal state. After this, we also analyzed the effect of gas concentration for oxidizing and reducing. In both the cases we start our analysis with no gas concentration. Memristance of the device changes with various gas concentration for both oxidizing and reducing type of gas as shown in Fig. 7a & 7b. Since in this context we are neglecting any transit time of the sensing process, we considered the ON-resistance of the device as instantly modified by the gas presence. With oxidizing gas concentration, resistance of the device decreases from the initial value and it further decreases as we increase the gas concentration. On the other way, for reducing gas concentration the resistance of the device increases from the initial value and it further increases with increase the gas concentration. In Fig. 7a & 7b, the resulting currents (with different colors) and with respect to the applied voltage show the switching behavior of the device and the variation of resistance for the incremental variation in concentration of oxidizing gas and reducing gas respectively. Comparing the plots, we can visualize the slope of the I-V characteristic in the ON state i.e. R_{on} resistance for the memristor device constantly changes linearly for the oxidising gas and non-linearly changes for reducing gases which are the result of our assumptions and is shown in Fig. 7a & 7b respectively. We reserve to verify these dependencies when we will have an experimental basis. The resistance may be read with several methods for example a voltage divider or a Wheatstone bridge, in order to obtain an index of the quantity of present gas. It is obvious that during this operation the stimulus voltage is within the PTV and the NTV.

B. Gas detection and sensitivity in CRS sensing

SPICE model based on VTEAM functionality for the memristor will provide the flexibility and high accuracy for gas sensing application. Our approach for CRS gas sensing is

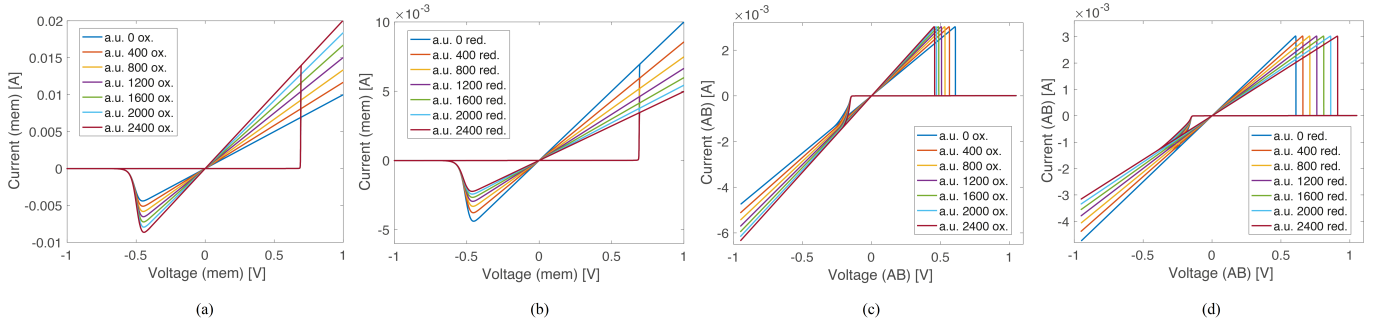


Figure 7: I-V curve showing variation in the ON-state resistance R_{on} by applying different concentrations of gases to the memristor sensor device: (a) Oxidising gas (b) Reducing gas. Multiple setting processes of the CRS cell, where the resistance of the sensitive memristor is modified by different a. u. gas: (c) Oxidising gas (d) Reducing gas.

based on the changing the resistive behavior of CRS device. In our simulation for CRS sensing, we consider sensing through a single memristor called A, and another memristor used for the minimizing sneak path current called B, as both these memristor connected back to back and perform as a CRS device in the array [17]. Our previous study in [17] shows the effectively minimization of sneak current in the CRS sensing architecture. Here, we report an analysis of how the total resistance of the cells (Memristors in CRS configuration) is changed due to gas and visualizing these variations in the I-V plot of the setting process of the cells in the memristive CRS sensing architecture. CRS sensing architecture shown in Fig. 3, read operation of a selected cell can be performed by providing the read voltage to the row of the selected cell and grounding the corresponding column by a load resistance [26]. Also, the read voltage is sufficiently low such that it can not alter the state of the memristors. In the case for sensing, evaluation of the sensor's response to the present gas is obtained by measuring the voltage drop on the load resistance R_L , as it forms a voltage divider with the sensing memristor (SM) and the access memristor (AM). In this case, I-V characteristic of the memristors pair will not be the same as shown before in Fig. 2 even if the reference circuit and the notations are the same. The difference in trend in I-V characteristic [17] for CRS within the array has been observed where memristor 2 (in Fig. 2) never reaches the HRS state during setting processes and presented in Fig. 7c & 7d.

Fig. 7c and 7d describe the aforementioned situations of interaction with different concentrations of gases by following the same trends in the I-V curve. Given that the cell constitutes a voltage divider, when the resistance of the SM varies, the value of V_{AB} at which the access memristor AM starts to switch from LRS to HRS is different. At the same time, when AM is in LRS, an increase in the SM resistance could make the latter subjected to a potential difference that erroneously sets it in HRS. However, this can be counteracted including appropriate noise margins for the stimuli provided, ensuring in this way correct operations. In this context, we do not involve the contribution of the external circuitry to the reading of the sensor's resistance. The current flowing through the cell I_{AB} is more sensitive to changes in SM resistance, the more the AM resistance is low. This is the reason why the sensitivity of the current to the gas is higher when AM is set in LRS and

not in HRS. The following equations quantify this concept:

$$I_{AB} = \frac{V_{AB}}{R_{on} + R_{on}(1 + \delta)} = \frac{V_{AB}}{R_{on}(2 + \delta)} \quad (7)$$

$$S_{\delta} = \left| \frac{dI_{AB}}{d\delta} \right| = \frac{V_{AB}}{R_{on}(2 + \delta)^2} \quad (8)$$

$$\text{if } \delta \ll 2, \quad S_{\delta} = \frac{V_{AB}}{4 \cdot R_{on}} \quad (9)$$

Where $\delta \cdot R_{on}$ is the amount of variation of the SM resistance and S_{δ} is the sensitivity of I_{AB} to δ . We can ascertain from equation (8) & (9), aside from strongly contrasting the influence of sneak currents, the role of AM (set in LRS for the selected cell and in HRS for the disconnected cells) also provides a great internal sensitivity to the circuit. This S_{δ} can eventually be amplified with the implementation of a suitable peripheral circuitry.

Taking in exam the formula in equation (8), we may consider to decrease the R_{on} value of the AM in order to increase the S_{δ} , but in this way, it may become extremely complex to control that resistance during setting processes. Although the threshold voltages of the single device remain the same, the value of the total applied voltage for which the access memristor changes state is different for different concentrations of gases. From the voltage divider formula, still being consistent with Fig. 2 labels:

$$V_{AM} = \frac{V_{AB}}{R_{AM} + R_{SM}} \cdot R_{AM} \quad (10)$$

The voltage on the access memristor (V_{AM}), is the product of the current ($I_{AB} = V_{AB}/(R_{AM} + R_{SM})$) flowing through the resistance R_{AM} . When the two resistances are comparable, that is when both memristors are L (on), the current I_{AB} is subject to the variations of R_{SM} because of gas. Therefore, this gives different V_{AM} for the same V_{AB} imposed. Also from this analysis, we can conclude that when R_{SM} decreases, namely when large concentrations of oxidising gases are present, it is difficult to reveal them. Because the access memristor in on state will exhibit a resistance higher than that of the sensor. Bounding I_{AB} to a small variable range. All these constrains will be taken in to account in future work in order to an accurate analysis of multi sensing using memristors.

IV. CONCLUSIONS

This paper analyzed the state change behaviour of memristor device in complementary resistive switch (CRS) configuration in multi-sensing architecture, when this architecture was exposed to the oxidizing and reducing gas environment. A translation of the VTEAM model in SPICE, and its modification for sensing has been presented in simplified manner and compared to the previously reported sensing models. This memristor model has been used for the investigation of CRS paradigm for gas sensing application. Reported simulation results show that the CRS characteristics would substantially improve the potential for memristor based sensing by eliminating sneak path currents with high density array.

APPENDIX

The SPICE code of the VTEAM model modified for sensing is given below. Several sets of parameters can be found in [19]. Recall to invert the values of v_{on} and v_{off} .

```
*VTEAM SPICE model modified for sensing
.SUBCKT VTEAM_SENS TE BE XSV C

.params Ron Roff alphaoff alphaon von voff
+koff kon xoff xon xinit p beta A

*Function D(x,v) - State Variable motion
.func D(V1,V2) = IF (V2 >= voff, IF(V2 <= von
+,0,kon*pow((V2/von-1),alphaon)*f(V1,V2)),
+koff*pow((V2/voff-1),alphaoff)*f(V1,V2))

*Reff function for reducing gas
.func Reff(V3) = Ron*(1+A*pow(V3,beta))

*Reff function for oxidising gas
*.func Reff(V3) = Ron/(1+A*pow(V3,beta))

*Assignment of the initial state variable
.ic V(XSV) = xinit

*Capacitance to determine the state variable
Cx XSV 0 {1}

* Biolek Window Function
.func f(V1,V2)=1-pow(((V1-xon)/(xoff-xon)-stp(V2)),(2*p))

*Current source to determine the state variable
Gx 0 XSV value = {D(V(XSV,0),V(TE,BE))}

*Conductance function
.func G(V1,V3) = pow((Reff(V3)+
+(Roff-Reff(V3))*(V1-xon)/(xoff-xon)), -1)

* Current source for memristor IV response
Gm TE BE value = {G(V(XSV,0),V(C,0))*V(TE,BE)}

*End of the model
.ENDS VTEAM_SENS
```

REFERENCES

- [1] L. Chua, "Memristor—the missing circuit element," *IEEE Transactions on circuit theory*, vol. 18, no. 5, pp. 507–519, 1971.
- [2] D. B. Strukov, G. S. Snider, D. R. Stewart, and R. S. Williams, "The missing memristor found," *nature*, vol. 453, no. 7191, pp. 80–83, 2008.
- [3] J. Cong and B. Xiao, "mrfpga: A novel fpga architecture with memristor-based reconfiguration," in *2011 IEEE/ACM international symposium on Nanoscale Architectures*. IEEE, 2011, pp. 1–8.
- [4] M. Ottavi, V. Gupta, S. Khandelwal, S. Kvatinsky, J. Mathew, E. Martinelli, and A. Jabir, "The missing applications found: Robust design techniques and novel uses of memristors," in *2019 IEEE 25th International Symposium on On-Line Testing and Robust System Design (IOLTS)*. IEEE, 2019, pp. 159–164.
- [5] V. Gupta, G. Lucarelli, S. Castro, T. Brown, and M. Ottavi, "Perovskite based low power synaptic memristor device for neuromorphic application," in *2019 14th International Conference on Design & Technology of Integrated Systems In Nanoscale Era (DTIS)*. IEEE, 2019, pp. 1–6.
- [6] C. L. Palson, D. D. Krishna, J. Mathew, B. R. Jose, M. Ottavi, and V. Gupta, "Memristor based adaptive impedance and frequency tuning network," in *2018 13th International Conference on Design & Technology of Integrated Systems In Nanoscale Era (DTIS)*. IEEE, 2018, pp. 1–2.
- [7] J. J. Yang, M. D. Pickett, X. Li, D. A. Ohlberg, D. R. Stewart, and R. S. Williams, "Memristive switching mechanism for metal/oxide/metal nanodevices," *Nature nanotechnology*, vol. 3, no. 7, pp. 429–433, 2008.
- [8] A. A. Haidry, A. Ebach-Stahl, and B. Saruhan, "Effect of pt/tio2 interface on room temperature hydrogen sensing performance of memristor type pt/tio2/pt structure," *Sensors and Actuators B: Chemical*, vol. 253, pp. 1043–1054, 2017.
- [9] N. S. M. Hadis, A. Abd Manaf, S. H. Herman, and S. H. Ngalm, "High roff/ron ratio liquid based memristor sensor using sol gel spin coating technique," in *2015 IEEE SENSORS*. IEEE, 2015, pp. 1–4.
- [10] M. Vidiš, T. Plecenik, M. Moško, S. Tomašec, T. Roch, L. Satrapinsky, B. Grančič, and A. Plecenik, "Gasistor: A memristor based gas-triggered switch and gas sensor with memory," *Applied Physics Letters*, vol. 115, no. 9, p. 093504, 2019.
- [11] T. Plecenik, M. Moško, A. Haidry, P. Đurina, M. Truchlý, B. Grančič, M. Gregor, T. Roch, L. Satrapinsky, A. Mošková *et al.*, "Fast highly-sensitive room-temperature semiconductor gas sensor based on the nanoscale pt–tio2–pt sandwich," *Sensors and Actuators B: Chemical*, vol. 207, pp. 351–361, 2015.
- [12] J. Bai and B. Zhou, "Titanium dioxide nanomaterials for sensor applications," *Chemical reviews*, vol. 114, no. 19, pp. 10131–10176, 2014.
- [13] A. Adeyemo, J. Mathew, A. Jabir, C. Di Natale, E. Martinelli, and M. Ottavi, "Efficient sensing approaches for high-density memristor sensor array," *Journal of Computational Electronics*, vol. 17, no. 3, pp. 1285–1296, 2018.
- [14] E. Linn, R. Rosezin, C. Kügeler, and R. Waser, "Complementary resistive switches for passive nanocrossbar memories," *Nature materials*, vol. 9, no. 5, pp. 403–406, 2010.
- [15] A. Adeyemo, A. Jabir, J. Mathew, E. Martinelli, C. Di Natale, and M. Ottavi, "Reliable gas sensing with memristive array," in *2017 IEEE 23rd International Symposium on On-Line Testing and Robust System Design (IOLTS)*. IEEE, 2017, pp. 244–246.
- [16] V. Gupta, S. Khandelwal, B. Raj, and R. Gupta, "Process variability aware low leakage reliable nano scale double-gate-finfet sram cell design technique," *Journal of Nanoelectronics and Optoelectronics*, vol. 10, no. 6, pp. 810–817, 2015.
- [17] D. Pellegrini, M. Ottavi, E. Martinelli, and C. Di Natale, "Complementary resistive switch sensing," in *2018 IEEE International Symposium on Defect and Fault Tolerance in VLSI and Nanotechnology Systems (DFT)*. IEEE, 2018, pp. 1–5.
- [18] S. Khandelwal, A. Bala, V. Gupta, M. Ottavi, E. Martinelli, and A. Jabir, "Fault modeling and simulation of memristor based gas sensors," in *2019 IEEE 25th International Symposium on On-Line Testing and Robust System Design (IOLTS)*. IEEE, 2019, pp. 58–59.
- [19] S. Kvatinsky, M. Ramadan, E. G. Friedman, and A. Kolodny, "Vteam: A general model for voltage-controlled memristors," *IEEE Transactions on Circuits and Systems II: Express Briefs*, vol. 62, no. 8, pp. 786–790, 2015.
- [20] Z. Birolek, D. Birolek, and V. Biolkova, "Spice model of memristor with nonlinear dopant drift," *Radioengineering*, vol. 18, no. 2, 2009.
- [21] Y. Yang, J. Mathew, R. A. Shafik, and D. K. Pradhan, "Verilog-a based effective complementary resistive switch model for simulations and analysis," *IEEE Embedded Systems Letters*, vol. 6, no. 1, pp. 12–15, 2013.
- [22] S. Kvatinsky, E. G. Friedman, A. Kolodny, and U. C. Weiser, "Team: Threshold adaptive memristor model," *IEEE transactions on circuits and systems I: regular papers*, vol. 60, no. 1, pp. 211–221, 2012.
- [23] S. Kvatinsky, D. Belousov, S. Liman, G. Satat, N. Wald, E. G. Friedman, A. Kolodny, and U. C. Weiser, "Magic—memristor-aided logic," *IEEE Transactions on Circuits and Systems II: Express Briefs*, vol. 61, no. 11, pp. 895–899, 2014.
- [24] Y. N. Joglekar and S. J. Wolf, "The elusive memristor: properties of basic electrical circuits," *European Journal of physics*, vol. 30, no. 4, p. 661, 2009.
- [25] C. Yakopcic, T. M. Taha, G. Subramanyam, R. E. Pino, and S. Rogers, "A memristor device model," *IEEE electron device letters*, vol. 32, no. 10, pp. 1436–1438, 2011.
- [26] C. Yakopcic, T. M. Taha, G. Subramanyam, and R. E. Pino, "Memristor spice model and crossbar simulation based on devices with nanosecond switching time," in *The 2013 International Joint Conference on Neural Networks (IJCNN)*. IEEE, 2013, pp. 1–7.